

Special
Collection

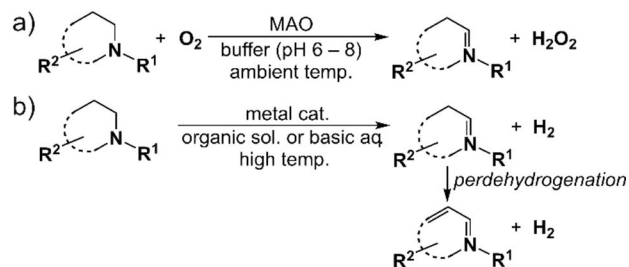
A Visible-Light Promoted Amine Oxidation Catalyzed by a Cp*Ir Complex

Holly Jane Davis,^[a] Daniel Häussinger,^[b] Thomas R. Ward,^{*[a]} and Yasunori Okamoto^{*[a, c]}

Through a rapid screening of Cp*Ir complexes based on a turn-on type fluorescence readout, a [Cp*Ir(dipyrido[3,2-a:2',3'-c]phenazine)Cl]⁺ complex was found to catalyze the blue-light promoted dehydrogenation of *N*-heterocycles under physiological conditions. In the dehydrogenation of tetrahydroisoquinolines, the catalyst preferentially yielded the monodehydrogenated product, accompanying H₂O₂ generation. We surmise that this mechanism may be reminiscent of flavin-dependent oxidases.

Monoamine oxidase (MAO) is a flavin-dependent enzyme that catalyzes the oxidation of a wide range of amines, including *N*-heterocycles, using molecular oxygen as a terminal oxidant (Scheme 1a). *N*-heterocycles are ubiquitous compounds widely represented in active pharmaceutical ingredients (APIs). Hence, MAOs have been engineered to improve their substrate scope, selectivity, and stability for industrial purposes.^[1]

To complement enzymes, organometallic catalysts have been developed for the dehydrogenation of *N*-heterocycles.^[2,3] To drive the oxidation of amines to completion, most organometallic catalysts require a sacrificial hydrogen acceptor, an undesirable feature from an atom-economical perspective.^[4]



Scheme 1. Dehydrogenations of *N*-heterocycles catalyzed by (a) monoamine oxidase (MAO) and (b) metal complexes.

Pioneering efforts in catalytic acceptorless dehydrogenation (CAD) have been reported by Yamaguchi and Fujita,^[5-7] Xiao,^[8,9] and Crabtree^[10] using Cp*Ir(III) pianostool- and cationic iridium complexes (Scheme 1b). CAD requires no external sacrificial oxidant and releases dihydrogen as sole by-product. Although great progress has been achieved,^[11-18] most of the CADs are carried out in organic solvent or under strongly alkaline conditions at high temperature. Noteworthy exceptions include work by Li^[19] and Kanai's^[20,21] tandem catalysis as well as Crabtree's^[22] electrocatalysis. In the context of H₂-storage, it may be advantageous to fully dehydrogenate the *N*-heterocycles, thus maximizing the hydrogen-gravimetric capacity. For API synthesis however, the perdehydrogenation may be a drawback (Scheme 1b). For example, tetrahydroharmine, harmaline, and harmine, are all naturally occurring *N*-heterocyclic alkaloids sharing the β-carboline structure, differing only in their degree of saturation but displaying different pharmacological properties.^[23] MAO selectively catalyzes only the first oxidation step, whereas CAD generally results in the fully perdehydrogenated product.^[5-22]

From the viewpoint of sustainable chemistry, a synthetic catalyst working in water under mild conditions is in high demand to reduce its environmental impact.^[24] Moreover, such a synthetic catalyst is also applicable to chemoenzymatic multistep transformation enabled by concurrent use of synthetic catalysts and enzymes.^[25] Here, we report on our efforts to develop an organometallic catalyst for the selective monodehydrogenation of *N*-heterocycles under mild conditions, comparable to those of typical enzymatic transformations.

As MAO plays an important role in maintaining homeostasis of neurotransmitters, the pro-fluorescent substrate **1** has been widely used to monitor its activity (Scheme 2a).^[26] We were pleased to find that the caged umbelliferone substrate **1** can be also used as a turn-on probe to the catalyst's dehydrogenation activity. Upon dehydrogenation of the *N*-heterocycle, the

[a] Dr. H. J. Davis, Prof. T. R. Ward, Prof. Y. Okamoto
Department of Chemistry
University of Basel
Mattenstrasse 24a
BRP 1096
Rosental CH-4058 Basel (Switzerland)
E-mail: thomas.ward@unibas.ch
yasunori.okamoto@tokohu.ac.jp

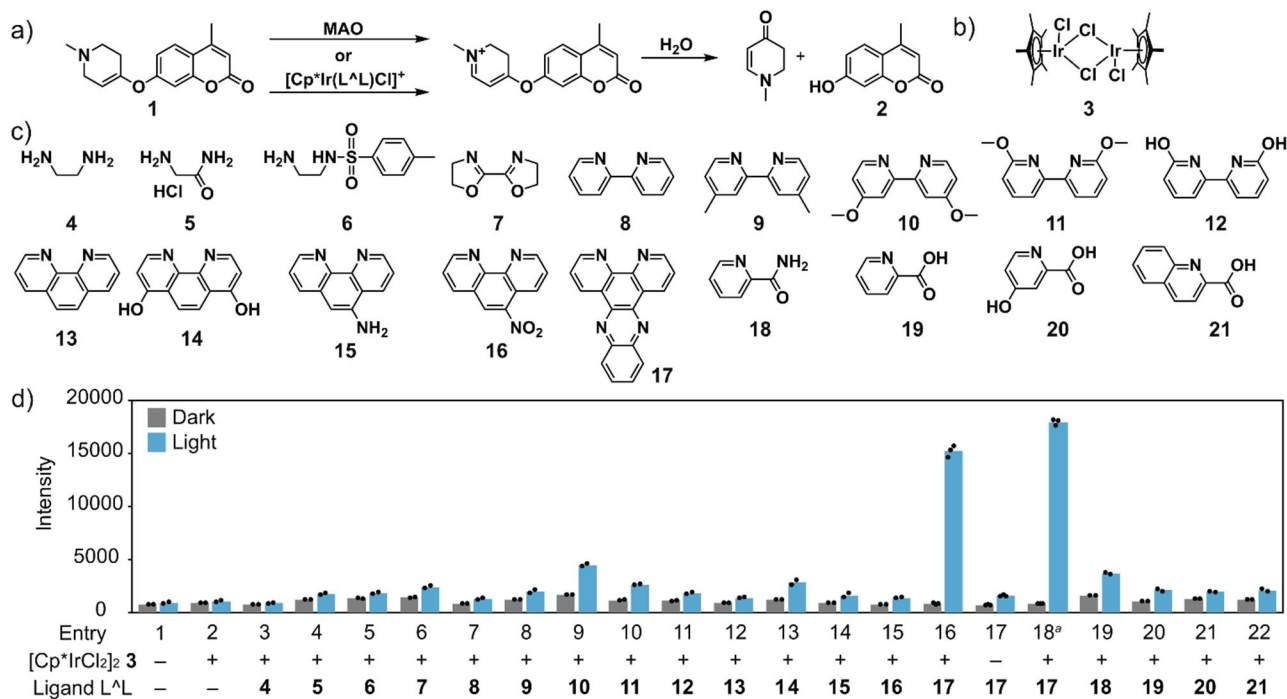
[b] Dr. D. Häussinger
Department of Chemistry
University of Basel
St. Johannis-Ring 19
CH-4056 Basel (Switzerland)

[c] Prof. Y. Okamoto
Frontier Research Institute for Interdisciplinary Sciences
Tohoku University
6-3 Aramaki aza Aoba
Aoba-ku
Sendai, 980-8578 (Japan)

Supporting information for this article is available on the WWW under <https://doi.org/10.1002/cctc.202000488>

This publication is part of the Young Researchers Series. More information regarding these excellent researchers can be found on the ChemCatChem homepage.

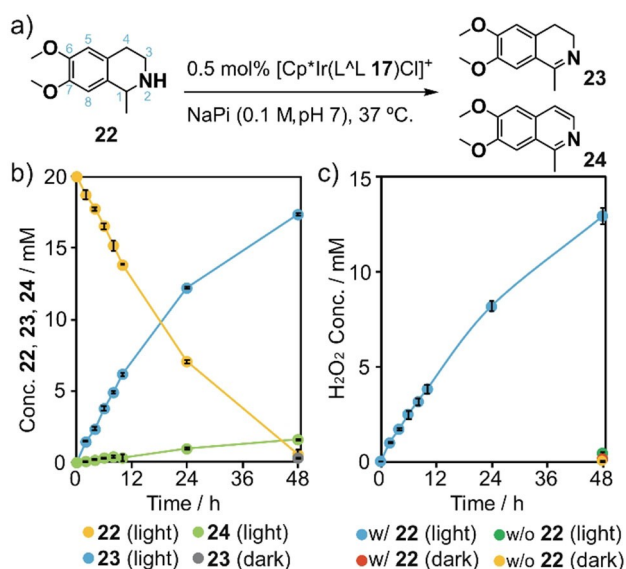
© 2020 The Authors. Published by Wiley-VCH Verlag GmbH & Co. KGaA, Weinheim. This is an open access article under the terms of the Creative Commons Attribution-NonCommercial License, which permits use, distribution and reproduction in any medium, provided the original work is properly cited and is not used for commercial purposes.



Scheme 2. (a) A turn-on type fluorescent probe **1** to detect MAO activity. Screening of catalytic activities of *in situ* formed complexes comprised of (b) [Cp*IrCl₂]₂ **3**, and (c) bidentate ligands **4**–**21**, (d) relying on the uncaging of the probe **1** upon amine oxidation. Reaction conditions: 50 μM [Cp*IrCl₂]₂ **3**, 110 μM Ligand **4**–**21** and 2 mM fluorescent probe **1** in PBS at 37 °C for 24 h. [a] An isolated [Cp*Ir(L^AL **17**)Cl](CF₃SO₃) (100 μM) was used. Fluorescence intensities (excitation at 320 nm and emission at 450 nm) of reaction mixtures in a 96-well plate are measured by a plate reader. Each value and average values of duplicate (entries 1–15, 19–22) and triplicate (entries 16–18) are displayed as dots and bars respectively.

fluorescent coumarin moiety **2** is uncaged, allowing the evaluation of catalytic activity. This strategy enabled us to conveniently screen Cp*Ir-based catalysts for the dehydrogenation of substrate **1**. Commercially-available bidentate ligands L^AL **4**–**21** (5.5 mol%) were screened in the presence of [Cp*IrCl₂]₂ **3** (2.5 mol%) in phosphate-buffered saline (PBS, pH 7.4) containing 5% DMSO at 37 °C (Scheme 2b, c). After 24 h, an aliquot (2 μl) was diluted with PBS (198 μl) in a 96-well plate, and the corresponding catalytic activity was determined by fluorescence (excitation at 320 nm and emission at 450 nm). Unexpectedly, none of the ligands displayed a significant increase in fluorescence compared to the negative control (Scheme 2d, grey bars). Inspired by Miller's work on the photo-acceleration of CAD catalyzed by [Cp*Ir(L^AL **8**)Cl]⁺ and [Cp*Ir(L^AL **10**)Cl]⁺,^[27] we repeated the screening in a photoreactor equipped with ca. 0.25 W blue LEDs (Scheme 2d, blue bars). Gratifyingly, the dipyrido[3,2-a:2',3'-c]phenazine **17** (Scheme 2d, entry 16) yielded the highest activity under photo-irradiation. Increased fluorescence was also observed for ligands L^AL **10**, **11**, **14**, and **18** (Scheme 2d, entries 9, 10, 13, and 19). Almost no enhancement was observed for either [Cp*IrCl₂]₂ **3** or L^AL **17** alone, suggesting that the [Cp*Ir(L^AL **17**)Cl]⁺ complex, formed *in situ*, is the active catalyst (Scheme 2d, entries 2, 17, and 16). To determine its catalytic performance, complex [Cp*Ir(L^AL **17**)Cl]⁺ was synthesized (Figure S1).^[28,29] Compared to the *in situ*-formed complex, the isolated complex displayed slightly improved activity (Scheme 2d, entries 16 and 18), which suggests that the *in situ* complexation is nearly quantitative.

As a benchmark reaction, we selected the dehydrogenation of salsolidine **22** (1-methyl-6,7-dimethoxy-1,2,3,4-tetrahydroisoquinoline, Scheme 3a), a natural alkaloid. While no conversion was observed under dark conditions, photo-irradiation promoted the reaction, leading to nearly quantitative consumption of the starting material **22** after 48 h, (Scheme 3b and Figure S2). The dehydrogenated product **23** and the perdehydrogenated product **24** were formed in 87% and 8% yield respectively. It was again confirmed that L^AL **17** alone does not catalyze this reaction. As H-abstraction from the amine can occur from either of the 1 or 3-position of amine **22**. Abstraction at the *N*-α benzylic site, 1-position, will generate a significantly more stable radical than that at the competing 3-position, leading to the observed major product **23**. The generation of **24**, on the other hand, can proceed via two pathways: either via the less favourable abstraction at the alternative site, tautomerisation and a second, favored, dehydrogenation event, or from direct tautomerisation from **23** before the second dehydrogenation. Potential interconversion of imine **23** and its isomer 1,4-dihydroisoquinolines is proposed to be mediated by a transient Cp*Ir–H species (Figure S3).^[8] As the ratio **23**:**24** does not vary over the course of the reaction, this suggests that [Cp*Ir(L^AL **17**)Cl]⁺ cannot reversibly convert **23** and 1,4-dihydroisoquinoline. We thus hypothesize that the commonly observed Cp*Ir–H species is not formed during this catalytic cycle.^[6,8,30,31] The limited formation of the perdehydrogenated product **24** may arise from the disfavored H-abstraction at the *N*-adjacent 3-position or benzylic 4-position of amine **22**. This is supported



Scheme 3. Time-course evolution of (a, b) the dehydrogenation of salsolidine **22** and (c) H₂O₂ catalyzed by [Cp*Ir(L^LL 17)Cl]⁺. Experimental conditions: 100 μM [Cp*Ir(L^LL 17)Cl]⁺, 20 mM salsolidine **22** in 100 mM NaPi (pH 7.0) at 37 °C under single blue LED irradiation. Concentrations of **22–24** were determined by ¹H-NMR spectroscopy by using 1,3,5-trimethoxybenzene as an internal standard. H₂O₂ was quantitated by HRP colorimetric assay. Average values and standard deviation for triplicate reactions are displayed.

by the fact that the dehydrogenation of imine **23** gave **24** with 12% yield, comparable to the yield of perdehydrogenated product **24** obtained upon dehydrogenation of amine **22** (8%, Scheme 3b). Indeed, scrutiny of the ¹H-NMR spectrum (Figure S4), revealed no hydride signal (typically found around –11 to –15 ppm). This is consistent with the preferential formation of the mono-dehydrogenated product **23**. We thus hypothesize that the reaction proceeds instead via a radical-based mechanism.

To probe whether atmospheric oxygen may be the terminal hydrogen acceptor, the presence of hydrogen peroxide was investigated. For this purpose, H₂O₂ was quantified using horseradish peroxidase (HRP) and 2,2'-azino-bis(3-ethylbenzothiazoline-6-sulfonic acid) (ABTS) to afford a characteristic increase in absorbance at 405 nm.^[32] As highlighted in Scheme 3b, the generation of H₂O₂ neatly reflects the oxidation of salsolidine **22** when the reaction is performed under air.

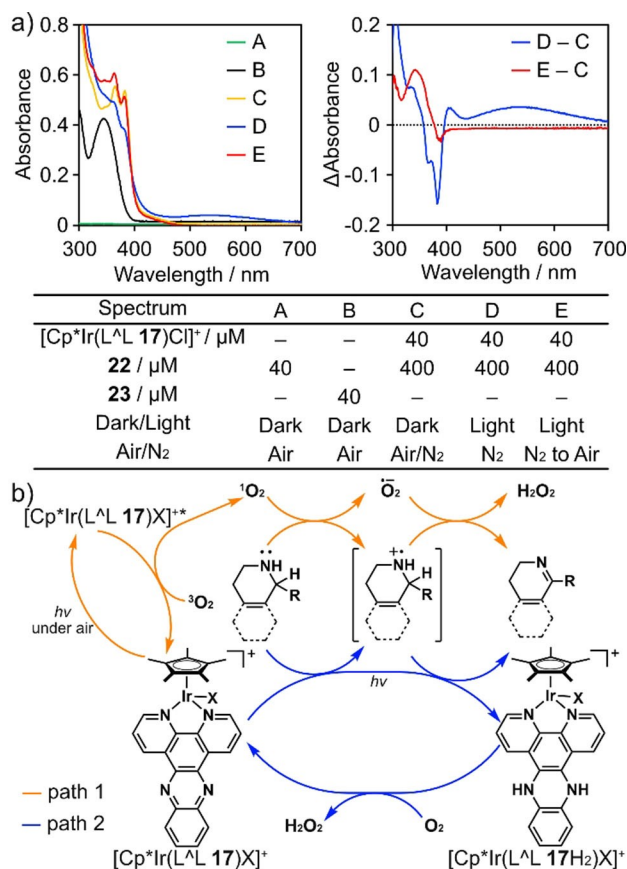
To gain further mechanistic insight, we carried out the dehydrogenation of substrate **22** in the presence of TEMPO (Table 1). Addition of excess TEMPO decreased the conversion by a factor of three. Taken together with the fact that

Entry	TEMPO	Under Air/N ₂	23 [%]	24 [%]
1	–	Air	78	8
2	40 mM	Air	25	15
3	–	N ₂	30	3

[a] Experimental details as listed in Scheme 3, with a reaction time = 45 h.

substoichiometric amounts of TEMPO shut down the reactivity of Ir–H species,^[33] it is suggested that catalytically-generated ¹O₂ and/or radical species may be involved. This conclusion is reached because TEMPO is known to mediate the conversion of the superoxide radical anion to H₂O₂^[34] but also to trap radical species and react with ¹O₂ which would unproductively deplete the finite oxygen supply. Accordingly, experiments carried out in the presence of 9,10-dimethylantracene, as a ¹O₂ trap, suggest that [Cp*Ir(L^LL 17)X]⁺ may sensitize O₂ likely due to the extended aromatic nature of L^LL 17 and the generated ¹O₂ may play a role as an active oxidizing species (Table S5 and path1 in Scheme 4b).

To confirm the involvement of oxygen in the mechanism, an anaerobic reaction was performed. Unexpectedly, conversion was observed under these conditions, albeit to a lesser extent: ~38% conversion under aerobic conditions (Table 1). We hypothesized that the cosolvent, DMSO present in 5% v/v may act as the oxidizing agent in the absence of dioxygen as observed by Das and coworkers.^[35] Substituting DMSO with DMF however, led to conversion both with and without dioxygen (Table S7). We assume that, in the absence of oxygen, the reaction proceeds via an alternative mechanism. One of the possible explanations is generation of H₂ instead of H₂O₂, like a typical CAD-type pathway. However, the unambiguous detection of H₂ under our experimental set-up proved challenging.



Scheme 4. (a) UV-vis spectra and their differential spectra of [Cp*Ir(L^LL 17)Cl]⁺ under different conditions. (b) Proposed mechanism.

Under anaerobic conditions, no resonance in the iridium hydride region was observed by $^1\text{H-NMR}$ spectrum, despite repeated efforts (Figure S4). While this does not preclude the possibility of a transient Ir–H species, the marked preference of mono- vs. perdehydrogenation suggests an alternative pathway. During these investigations, an air-sensitive blue complex was observed, which was scrutinized by UV-vis and NMR spectroscopy (Scheme 4a and see discussion in the page S23 for the emission studies).

Upon photoirradiation under anaerobic conditions, absorption from 435 to 700 nm increased and the $^1\text{H-NMR}$ resonances for $\text{L}^{\wedge}\text{L}$ **17** were shifted upfield, leading us to suggest that this species is $[\text{Cp}^*\text{Ir}(\text{L}^{\wedge}\text{L} \text{17H}_2)\text{X}]^+$, whereby the ligand **17** has been reduced across the heteroaromatic ring (Scheme 4b, Figure S5 and S7–S10).^[36–38] The blue complex remains moderately stable under nitrogen for >1 week without an increase in consumption of amine **22**. This leads us to suggest that intermediate $[\text{Cp}^*\text{Ir}(\text{L}^{\wedge}\text{L} \text{17H}_2)\text{X}]^+$ requires photoexcitation to be turned over (Figure S6).

When exposed to air, $[\text{Cp}^*\text{Ir}(\text{L}^{\wedge}\text{L} \text{17H}_2)\text{X}]^+$ produced a single species. Based on $^1\text{H-NMR}$ spectra, we conclude it most resembles the $[\text{Cp}^*\text{Ir}(\text{L}^{\wedge}\text{L} \text{1722})]^+$ (Figure S5). This suggests that the catalyst reduction is caused by an unbound equivalent of the amine substrate (Table S9). The differential spectrum (E–C, in Scheme 4a) reveals the production of imine **23** without affecting any other components during photoreduction and oxidation of the catalyst. Upon regeneration of the reduced catalyst by O_2 , $[\text{Cp}^*\text{Ir}(\text{L}^{\wedge}\text{L} \text{17H}_2)\text{X}]^+$ may act as a $2\text{e}^-/2\text{H}^+$ donor in the reduction of O_2 to produce H_2O_2 (path 2 in Scheme 4b).^[36] This mechanism is reminiscent of flavin-dependent oxidases. We thus tentatively propose an aerobic mechanism mediated by singlet oxygen, or a mechanism involving $\text{L}^{\wedge}\text{L}$ **17** reduction.

Next, $[\text{Cp}^*\text{Ir}(\text{L}^{\wedge}\text{L} \text{17})\text{Cl}]^+$ was tested for the reduction of *N*-heterocycles, derived either from tetrahydroisoquinoline or indoline **25–31** (Figure 1).^[39] Higher TON and selectivity correlate well with the stability of the C-centered radical with a modest contribution from steric hindrance, rendering the H

atom less accessible for abstraction. The acyclic substrate **32** was also oxidized and subsequently hydrolyzed. In analogy to substrates **25** and **27**, the amine oxidation seems to proceed at the less hindered *N*- α position. In all cases, however, the dehydrogenation product was formed preferentially over the perdehydrogenation product.

In summary, we have identified a visible light-promoted dehydrogenation catalyst, $[\text{Cp}^*\text{Ir}(\text{L}^{\wedge}\text{L} \text{17})\text{Cl}]^+$, which is active under physiological conditions. Depending on the presence or absence of O_2 , we surmise that the reaction proceeds via two competing reaction pathways. Detailed mechanistic studies are underway alongside the introduction of the reaction into a chemoenzymatic cascade.^[25]

Acknowledgements

The authors acknowledge Dr. Alessandro Prescimone, Mr. Adriano d'Addio and Mr. Daniel Joss for their help with the X-ray crystal structure analysis and NMR measurements. TRW acknowledges continued support from the Swiss National Science Foundation (grant 200020_182046), the NCCR Molecular Systems Engineering. HJD thanks the Marie Skłodowska-Curie H2020-MSCA-IF-2018 for a postdoctoral fellowship. YO thanks JST ACT-X (JPMJAX1913) and support from FRIS, Tohoku University.

Conflict of Interest

The authors declare no conflict of interest.

Keywords: Photocatalysis · Selective-dehydrogenation · Biomimetic · Reaction-in-water · Organometallic complex

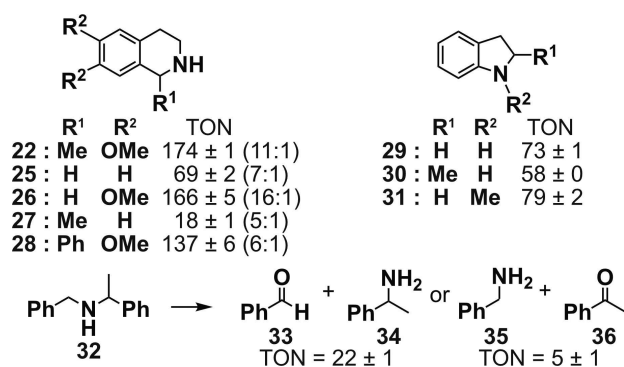


Figure 1. Photocatalytic dehydrogenation of *N*-heterocycles **22–31** and acyclic substrate **32** catalyzed by $[\text{Cp}^*\text{Ir}(\text{L}^{\wedge}\text{L} \text{17})\text{Cl}]^+$. Experimental conditions: 100 μM $[\text{Cp}^*\text{Ir}(\text{L}^{\wedge}\text{L} \text{17})\text{Cl}]^+$, 20 mM **22–32** in 100 mM NaPi (pH 7.0) at 37 °C under blue LED irradiation for 48 h in the presence of air. TONs are determined by $^1\text{H-NMR}$ by using an internal standard. Average values for triplicate reactions are displayed and mono vs. perdehydrogenation ratio shown in brackets.

- [1] V. F. Batista, J. L. Galman, D. C. G. A. Pinto, A. M. S. Silva, N. J. Turner, *ACS Catal.* **2018**, *8*, 11889–11907.
- [2] G. E. Dobreiner, R. H. Crabtree, *Chem. Rev.* **2010**, *110*, 681–703.
- [3] J. Choi, A. H. R. MacArthur, M. Brookhart, A. S. Goldman, *Chem. Rev.* **2011**, *111*, 1761–1779.
- [4] R. A. Sheldon, *J. R. Soc. Interface* **2016**, *13*, 1–7.
- [5] R. Yamaguchi, C. Ikeda, Y. Takahashi, K. Fujita, *J. Am. Chem. Soc.* **2009**, *131*, 8410–8412.
- [6] K. Fujita, Y. Tanaka, M. Kobayashi, R. Yamaguchi, *J. Am. Chem. Soc.* **2014**, *136*, 4829–4832.
- [7] K. Fujita, T. Wada, T. Shiraishi, *Angew. Chem. Int. Ed.* **2017**, *56*, 10886–10889; *Angew. Chem.* **2017**, *129*, 11026–11029.
- [8] J. Wu, D. Talwar, S. Johnston, M. Yan, J. Xiao, *Angew. Chem. Int. Ed.* **2013**, *52*, 6983–6987; *Angew. Chem.* **2013**, *125*, 7121–7125.
- [9] D. Talwar, A. G. de Castro, H. Y. Li, J. Xiao, *Angew. Chem. Int. Ed.* **2015**, *54*, 5223–5227; *Angew. Chem.* **2015**, *127*, 5312–5316.
- [10] M. G. Manas, L. S. Sharninghausen, E. Lin, R. H. Crabtree, *J. Organomet. Chem.* **2015**, *792*, 184–189.
- [11] C. Gunanathan, D. Milstein, *Science* **2013**, *341*, 1229712.
- [12] S. Chakraborty, W. W. Brennessel, W. D. Jones, *J. Am. Chem. Soc.* **2014**, *136*, 8564–8567.
- [13] R. Xu, S. Chakraborty, H. Yuan, W. D. Jones, *ACS Catal.* **2015**, *5*, 6350–6354.
- [14] M. Kojima, M. Kanai, *Angew. Chem. Int. Ed.* **2016**, *55*, 12224–12227; *Angew. Chem.* **2016**, *128*, 12412–12415.
- [15] Q. Yin, M. Oestreich, *Angew. Chem. Int. Ed.* **2017**, *56*, 7716–7718; *Angew. Chem.* **2017**, *129*, 7824–7826.
- [16] A. Vivancos, M. Beller, M. Albrecht, *ACS Catal.* **2018**, *8*, 17–21.

- [17] R. Wang, H. Fan, W. Zhao, F. Li, *Org. Lett.* **2016**, *18*, 3558–3561.
- [18] H. Fan, W. Zhang, W. Zhao, F. Li, *ChemistrySelect* **2017**, *2*, 5735–5739.
- [19] K. H. He, F. F. Tan, C. Z. Zhou, G. J. Zhou, X. L. Yang, Y. Li, *Angew. Chem. Int. Ed.* **2017**, *56*, 3080–3084; *Angew. Chem.* **2017**, *129*, 3126–3130.
- [20] S. Kato, Y. Saga, M. Kojima, H. Fuse, S. Matsunaga, A. Fukatsu, M. Kondo, S. Masaoka, M. Kanai, *J. Am. Chem. Soc.* **2017**, *139*, 2204–2207.
- [21] H. Fuse, M. Kojima, H. Mitsunuma, M. Kanai, *Org. Lett.* **2018**, *20*, 2042–2045.
- [22] O. R. Luca, D. L. Huang, M. K. Takase, R. H. Crabtree, *New J. Chem.* **2013**, *37*, 3402–3405.
- [23] H. Song, Y. Liu, Y. Liu, L. Wang, Q. Wang, *J. Agric. Food Chem.* **2014**, *62*, 1010–1018.
- [24] T. Kitanosono, K. Masuda, P. Xu, S. Kobayashi, *Chem. Rev.* **2018**, *118*, 679–746.
- [25] N. J. Turner, *Nature* **2018**, *560*, 310–311.
- [26] S. Long, L. Chen, Y. Xiang, M. Song, Y. Zheng, Q. Zhu, *Chem. Commun.* **2012**, *48*, 7164–7166.
- [27] S. M. Barrett, S. A. Slattey, A. J. M. Miller, *ACS Catal.* **2015**, *5*, 6320–6327.
- [28] D. Herebian, W. S. Sheldrick, *J. Chem. Soc. Dalton Trans.* **2002**, 966–974.
- [29] X. Duan, D. Liu, C. Chan, W. Lin, *Small* **2015**, *11*, 3962–3972.
- [30] Z. Liu, R. J. Deeth, J. S. Butler, A. Habtemariam, M. E. Newton, P. J. Sadler, *Angew. Chem. Int. Ed.* **2013**, *52*, 4194–4197; *Angew. Chem.* **2013**, *125*, 4288–4291.
- [31] S. Ogo, R. Kabe, H. Hayashi, R. Harada, S. Fukuzumi, *Dalton Trans.* **2006**, 4657–4663.
- [32] R. L. Peterson, J. W. Ginsbach, R. E. Cowley, M. F. Qayyum, R. A. Himes, M. A. Siegler, C. D. Moore, B. Hedman, K. O. Hodgson, S. Fukuzumi, E. I. Solomon, K. D. Karlin, *J. Am. Chem. Soc.* **2013**, *135*, 16454–16467.
- [33] N. Humbert, D. J. Vyas, C. Besnard, C. Mazet, *Chem. Commun.* **2014**, *50*, 10592–10595.
- [34] N. A. Romero, K. A. Margrey, N. E. Tay, D. A. Nicewicz, *Science* **2015**, *349*, 1326–1330.
- [35] D. Riemer, W. Schilling, A. Goetz, Y. Zhang, S. Gehrke, I. Tkach, O. Hollóczki, S. Das, *ACS Catal.* **2018**, *8*, 11679–11687.
- [36] K. Kobayashi, H. Ohtsu, K. Nozaki, S. Kitagawa, K. Tanaka, *Inorg. Chem.* **2016**, *55*, 2076–2084.
- [37] D. A. McGovern, A. Selmi, J. E. O'Brien, J. M. Kelly, C. Long, *Chem. Commun.* **2005**, 1402–1404.
- [38] B. König, R. Lechner, *Synthesis* **2010**, 1712–1718.
- [39] Under optimized conditions, it is suggested that substrates bearing benzylic or allylic N- α C–H can be oxidized.

Manuscript received: March 21, 2020
Revised manuscript received: June 11, 2020
Accepted manuscript online: June 12, 2020
Version of record online: July 22, 2020